

# Impact of CMS Multi-jets and Missing Energy Search on CMSSM Fits

---

**B C Allanach<sup>a</sup>**

<sup>a</sup>*DAMTP, CMS, University of Cambridge, Wilberforce Road, Cambridge CB3 0WA, United Kingdom*

*E-mail:* [B.C.Allanach@damtp.cam.ac.uk](mailto:B.C.Allanach@damtp.cam.ac.uk)

**ABSTRACT:** Recent CMS data significantly extend the exclusion limits for supersymmetry. We examine the impact of such data on global fits of the constrained minimal supersymmetric standard model (CMSSM) to indirect and cosmological data. By simulating supersymmetric signal events at the LHC, we construct a likelihood map for the recent CMS data, validating it against the exclusion region calculated by the experiment itself. A previous CMSSM global fit is then re-weighted by our likelihood map. The CMS results nibble away at the high fit probability density region, transforming probability distributions for the scalar and gluino masses. The CMS search has a non-trivial effect on  $\tan\beta$  due to correlations between the parameters implied by the fits to indirect data.

**KEYWORDS:** Supersymmetric Phenomenology, Markov chain Monte Carlo, Large Hadron Collider

---

## Contents

<b>1</b>	<b>Introduction</b>	<b>1</b>
<b>2</b>	<b>CMS <math>\alpha_T</math> Likelihood Map</b>	<b>3</b>
2.1	The $\alpha_T$ Search	3
2.2	Simulation of the SUSY signal	4
2.3	Validation of the SUSY signal	4
<b>3</b>	<b>Global CMSSM Fits Including the CMS <math>\alpha_T</math> Search</b>	<b>7</b>
<b>4</b>	<b>Summary and Conclusions</b>	<b>12</b>
<b>A</b>	<b>Validation of <math>\tan\beta - A_0</math> Independence of the Likelihood</b>	<b>12</b>

---

## 1 Introduction

Many recent efforts have examined whether various simple supersymmetric models are compatible with the anomalous magnetic moment of the muon, the dark matter relic density, direct searches for supersymmetric particles and Higgs bosons, and electroweak observables simultaneously [1–18]. Global fits take into account variations with respect to all of the parameters of the model that have a significant impact on the observables, including Standard Model (SM) parameters. Various algorithmic tools have now been developed to allow such a sampling of a multi-dimensional parameter space, which may be multi-modal [19–21]. However, current global fits of indirect and cosmological data to the CMSSM are not robust. This is shown by the large prior dependence of the Bayesian fits [2, 5, 7, 10]. Frequentist fits to edge measurements from hypothetical LHC SUSY edge measurements showed an incorrect confidence level (C.L.) coverage of frequentist fits when the C.L.s are calculated by assuming a  $\chi^2$  distribution [22]. There are no published coverage studies of global SUSY fits and, since they are expected to be less robust than fits to an LHC SUSY signal, a coverage study of the frequentist fits is necessary and long overdue. A fit to a large volume string model with only two free parameters additional to the SM (the ratio of the Higgs vacuum expectation values,  $\tan\beta$ , and an overall supersymmetry breaking mass scale) did display approximate prior independence [23]. On the other hand, a fit to a model with three parameters additional to the SM (minimal anomaly mediated supersymmetry breaking) showed significant prior dependence [24]. Fits to models with more than three additional parameters have also (so far) shown a lack of robustness [11, 13, 24, 25].

The LHC general purpose experiments ATLAS and CMS actively searched for supersymmetric states in 2010, collecting some  $\sim 35\text{pb}^{-1}$  of recorded collisions each at a center of mass energy  $\sqrt{s} = 7$  TeV. The first dedicated analysis of this data recently appeared

from CMS, examining multi-jet states accompanied by missing transverse momentum [26]. The data were statistically compatible with the SM predictions, allowing the experiment to place constraints on supersymmetry. In its publication, CMS also analyzed the CMSSM, showing that the equivalent previous best exclusion from experiments at LEP and the Tevatron are significantly surpassed. In 2011, some thirty times more luminosity is expected to be collected by the LHC experiments than in 2010 and, in the absence of a signal, the search reach will doubtless be extended significantly.

Here, we wish to examine the extent to which the first publicly available search from CMS impacts on the previous global supersymmetric fits. Despite the fact that such fits are not yet robust and therefore not definitive (and are likely to remain so until direct supersymmetric searches yield a significant signal), such an exercise should give interesting information on whether the good-fit region is being covered yet, and the prospects for searches in the near future. The effect of the CMS direct SUSY search on the fits may be qualitatively examined. We demonstrate how one can perform such an analysis in a reasonable amount of computational time, and hopefully set precedents for good practice, such as validation against CMS's more sophisticated event simulation. The CMS search has already been used to examine how much of the CMSSM parameter space is allowed beyond the 95% exclusion contour: [27], around 1% according to the author's metric related to the naturalness of electroweak symmetry breaking. We shall examine the effect of the search results on a previous Bayesian fit, because of the computational ease with which the impact of the direct search can be quantified (as opposed to the frequentist methods, where an examination of coverage would be necessary to set confidence levels, requiring many such fits). We pick the CMSSM as our model partly because CMS analyzed it explicitly in their publication. Thus, it is possible to check our evaluation of the CMS data, which includes various approximations and simplifications, against their more sophisticated treatment. We use the 95% confidence level exclusion contour in a two dimensional parameter plane that CMS provided in their paper. The CMSSM is a familiar model that many works have analyzed and it provides a well-defined playground for examining supersymmetric phenomenology, with only a few free parameters additional to the SM: the universal scalar mass  $m_0$ , the universal gaugino mass  $m_{1/2}$ , the supersymmetric (SUSY) breaking scalar trilinear coupling  $A_0$ ,  $\tan\beta$  and the sign of  $\mu$ , a parameter in the Higgs potential. Although the CMSSM is very specific and may well not represent the correct pattern of supersymmetry breaking, aspects of its phenomenology are similar to the class of models which are effectively perturbations around the CMSSM assumptions.

Early ATLAS jets plus missing transverse momentum data presented at Summer conferences in 2010 have already been used [28] to place bounds on simplified models containing squarks and gluinos which decay to jets and neutralinos. This analysis was based only on  $70 \text{ nb}^{-1}$  of data. This data is not used here because it is only a small integrated luminosity, with a small effect compared to the data we use. We shall see that the predicted CMS SUSY search signal is approximately independent of all parameters except  $m_0$  and  $m_{1/2}$ , which leads to significant simplifications in the incorporation of its results into the fits.

Our paper proceeds as follows: in section 2, we detail the CMS SUSY search and results, showing how we approximately reproduce their analysis, resulting in a likelihood

map on the CMSSM parameter space. We then go on to apply the approximate likelihood map to global CMSSM fits in section 3, showing how the fits change. We conclude in section 4. We calculate the accuracy of our approximation that the CMS SUSY signal is approximately independent of all parameters except  $m_0$  and  $m_{1/2}$  in Appendix A.

## 2 CMS $\alpha_T$ Likelihood Map

### 2.1 The $\alpha_T$ Search

In  $35\text{pb}^{-1}$  of  $pp$  collisions at  $\sqrt{s} = 7$  TeV at the CERN LHC, CMS examined events with significant transverse momentum  $|\mathbf{p}_T|$  in the jets  $j_i$  for multi-jet events, i.e.  $H_T = \sum_{i=1}^{N_{jet}} |\mathbf{p}_T^{j_i}| > 350$  GeV.  $\mathbf{p}_T^{j_i} = (p_x^{j_i}, p_y^{j_i})$  is the jet momentum transverse to the beam. Isolated lepton and photon vetoes were also applied. The final event selection relies on a variable  $\alpha_T$ , that is designed to discriminate effectively against QCD multi-jet production, where one of the jets' transverse momentum is significantly mis-measured [29], although it has been argued that the variable gives no special immunity to initial and final state radiation effects [30]. The system of  $N_j$  jets is reduced to a system of two jets by combining them into pseudo-jets  $A$  and  $B$ <sup>1</sup>. The combination chosen is the one that minimizes

$$\Delta H_T \equiv \sum_{j_i \in A} |\mathbf{p}_T^{j_i}| - \sum_{j_i \in B} |\mathbf{p}_T^{j_i}|. \quad (2.1)$$

One then calculates

$$\alpha_T = \frac{H_T - \Delta H_T}{2\sqrt{H_T^2 - \mathcal{H}_T^2}}, \quad (2.2)$$

where  $\mathcal{H}_T = \sqrt{(\sum_{i=1}^{N_{jet}} p_x^{j_i})^2 + (\sum_{i=1}^{N_{jet}} p_y^{j_i})^2}$  is defined at the jet-level. Note that often, a different definition of  $\alpha_T$  is given which is identical in the idealized case of massless di-jet events, but which differs from the result of Eq. 2.2 for the case of more than two jets. The cut  $\alpha_T > 0.55$  is used in CMS's analysis.

The jets are defined by the anti- $k_T$  algorithm with a size parameter of 0.5, a minimum  $|\mathbf{p}_T| > 50$  GeV and a bound on the pseudo-rapidity  $\eta$  of  $|\eta| < 3$ . The highest  $|\mathbf{p}_T|$  jet is required to have  $|\eta| < 2.5$  and the transverse momentum of the two leading jets must exceed 100 GeV.  $\mathbf{p}_T(cal)$  is defined over all calorimetric deposits of the event, and events with  $R_{miss} = \mathcal{H}_T/|\mathbf{p}_T(cal)| > 1.25$  are rejected to protect against multiple jets failing the  $|\mathbf{p}_T| > 50$  GeV requirement.

Additional experimental cuts to remove events where significant energy losses from jets going into un-instrumented regions were also placed. After all of these cuts,  $o = 13$  events on a predicted SM background of  $9.3 \pm 0.9$  were observed. This search is compatible with SM predictions at the  $2\sigma$  level, with a  $\sim 1\sigma$  slight excess of events.

---

<sup>1</sup>We note here that the difference between transverse momentum and transverse energy can be significant for pseudo-jets, even within an event generator, because they have effective masses. Like the authors of Ref. [31], we urge care when defining them.

## 2.2 Simulation of the SUSY signal

In order to simulate the production of sparticles from LHC  $pp$  collisions, we use `HERWIG++-2.4.2` [32], with the default underlying event model switched on. Supersymmetric spectra are generated with `SOFTSUSY3.1.7` [33], with decay branching ratios and widths calculated by `SDECAY` [34]. The information about supersymmetric masses, mixings, couplings and decays is transferred between the programs by the SUSY Les Houches Accord [35]. `fastjet-2.4.1` [36] is used to define the jets in the anti- $k_T$  scheme with  $R = 0.5$  in the energy recombination scheme. The cuts mimic those of the experiment and are summarized in Eq. 2.3:

$$H_T > 350 \text{ GeV}, |\mathbf{p}_T^{j_2}| > 100 \text{ GeV}, \alpha_T > 0.55, R_{\text{miss}} < 1.25, l \text{ isolation.} \quad (2.3)$$

The lepton isolation veto (‘ $l$  isolation’) is implemented as follows<sup>2</sup>: any events with leptons that have less than 10 GeV of  $|\mathbf{p}_T|$  in a cone of  $\Delta R = \sqrt{(\Delta\eta)^2 + (\Delta\phi)^2} < 0.3$  are vetoed, where  $\phi$  is azimuthal angle around the beam-line. For a given CMSSM parameter point predicting  $s$  supersymmetric events passing the cuts, we calculate the likelihood to be

$$\mathcal{L} = \frac{e^{-(s+b)}(s+b)^o}{o!} \quad (2.4)$$

from the Poisson distribution for the central value of the predicted number of signal  $s$  plus background events  $b = 9.3$ . We neglect the small uncertainty of 0.9 on  $b$ : in the next section, where we validate our calculation, we shall see that the effect of our approximations (including this one) are reasonable.

Our simulation of the signal is cruder than the CMS analysis: it is only leading order in QCD, whereas CMS’s includes next-to-leading order factors for the overall cross-section, and we have not performed a dedicated detector simulation to convolute the signal kinematic distributions with the detector response. Even had we included these effects, it would be important to check our approximations by reproducing CMS’s calculated signal because, being outside the collaboration, we do not have access to the full detector simulation. There is no need for us to validate the SM background, since we may use CMS’s predicted rates for it.

## 2.3 Validation of the SUSY signal

In order to validate our calculation of the signal and see that we are obtaining a reasonably accurate result despite our approximations, we first calculate the  $\alpha_T$  distribution in the di-jet and more than two jet channels for the CMSSM model point LM0 ( $m_0 = 200$  GeV,  $m_{1/2} = 160$  GeV,  $A_0 = -400$  GeV,  $\tan\beta = 10$  and  $\mu > 0$ ). The only cut we place for the purposes of this check is  $H_T > 350$  GeV, mimicking CMS. The distributions for the ‘di-jets’ and ‘three or more jets’ channels are shown in Fig. 1 for our simulation and for

---

<sup>2</sup>CMS uses a lepton isolation criterion involving tracks and energy deposits in calorimeter cells. Since we do not perform a detector simulation, we do not have access to simulated tracks and so we must deviate slightly from CMS’s lepton isolation criteria, although our criteria are very similar in effect. CMS’ lepton isolation criteria are: in  $\Delta R < 0.3$  around the lepton, the lepton is considered isolated if the scalar  $p_T$  sum of all of the tracks in the cone plus the  $|\mathbf{p}_T|$ s of the energy deposits in the calorimeter divided by the  $|\mathbf{p}_T|$  of the lepton candidate is larger than 0.15.

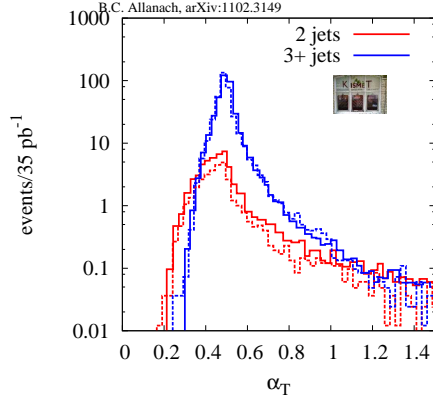


**Figure 1.** SUSY signal  $\alpha_T$  distributions for the LM0 point and  $\sqrt{s} = 7$  TeV in the di-jets channel and in the 3 or more jets channel, as displayed by the legend. Solid lines are obtained from Fig. 2 of Ref. [26]: the CMS signal simulation including next-to-leading order (NLO) corrections and full detector simulation whereas the dashed lines show the results of our simulation and approximations. The only cut applied is  $H_T > 350$  GeV.

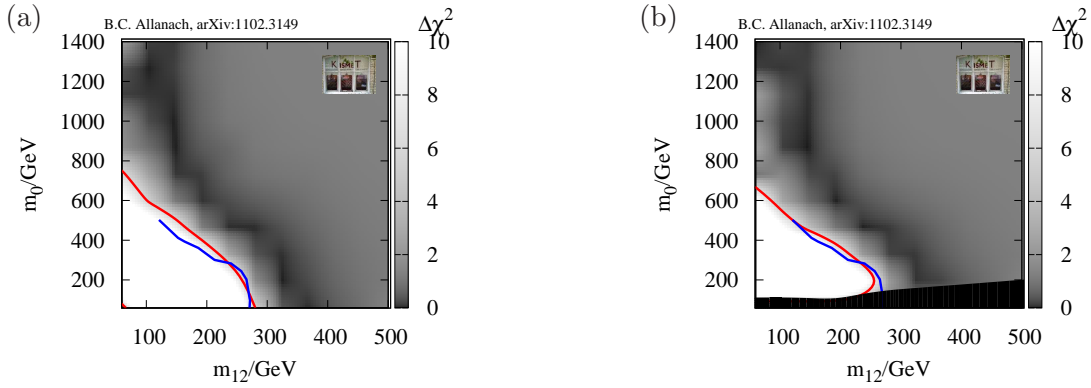


**Figure 2.** Our approximation to the CMS  $\alpha_T$ -search CMSSM likelihood map for (a)  $\tan\beta = 3$ ,  $A_0 = 0$ , (b)  $\tan\beta = 30$  and  $A_0 = -200$  GeV, where the blacked out region at the bottom denotes a  $\tilde{\tau}_1$  lightest supersymmetric particle. The region below the red (lighter) curve is excluded at 95% confidence level (C.L.), and  $\Delta\chi^2$  is clipped at 10. The CMS 95% C.L. curve is shown as the blue (darker) line.

CMS’ signal simulation. The figure verifies that our calculation of the  $\alpha_T$  distribution is compatible with the calculation of the experimental collaboration: the normalization of the sub-dominant exclusive two jets sample is slightly different, but the shapes of both samples match extremely well. After all of the other cuts are applied, including  $\alpha_T > 0.55$ , the acceptance times efficiency of the SUSY signal selection is 5.0%.

Next, we perform a scan over CMSSM parameter space to see how closely we can reproduce CMS’s calculation of the 95% contour. Like CMS, we choose  $\tan\beta = 3$  and  $A_0 = 0$  for this scan. At each point in an 11 by 11 grid, we simulate 10 000 SUSY events,

calculating  $\mathcal{L}$  from Eq. 2.4. We then calculate  $\Delta\chi^2 = -2\ln\mathcal{L}/\mathcal{L}(\text{max})$ , where  $\mathcal{L}(\text{max})$  is the maximum value of the likelihood over the plane.  $\Delta\chi^2$  is then interpolated between the grid points, and shown in Fig. 2a. The background colour density displays  $\Delta\chi^2$ , and is clipped at an upper value of 10. The light green solid curve is our predicted 95% C.L. lower bound, coming from the  $\Delta\chi^2 = 5.99$  contour. We compare this with the blue (darker) line, the published CMS contour for the full next-to-leading order observed limit. We see that despite our approximations, the contours for the expected sensitivity and the 95% C.L. limits agree reasonably well. Indeed, next-to-leading order corrections to the production cross-section will tend to increase the signal rate, whereas we expect detector effects to decrease it. Thus we expect that the two effects cancel to some extent. We conclude that we should be able to use the likelihood as calculated here, although we note that we would really like more likelihood information from the experiments far away from the 95% level contour so that we could validate our simulation more thoroughly. The  $\sim 1\sigma$  excess of observed events manifests as a dark valley of  $\chi^2 < 1$  in Fig. 2. This will have an effect on the CMSSM global fit, as we shall see.

For the  $\alpha_T$  search, where the signal involves just jets and missing transverse momentum, we expect the signal rate to be approximately independent of  $\tan\beta$  and  $A_0$ . This is because the signal is dominated by the strong cross-sections of squark and gluino production, which do not depend to any significant degree on those parameters. Third generation squark masses do depend upon  $A_0$  and  $\tan\beta$  to some extent, but the SUSY production cross-sections have a dominant component coming from the two lighter generations of squark and the gluino. The decay cascades of the first two generations of squarks and gluinos are likewise expected to be quite insensitive to  $A_0$  and  $\tan\beta$ , being dominated by strong processes until the decay into the lightest neutralino. Being able to model the dependence of the CMS  $\alpha_T$ -search likelihood on  $m_0$  and  $m_{1/2}$ , while ignoring the effect of  $A_0$  and  $\tan\beta$  leads to a significant simplification when we come to take it into account in our global CMSSM fits. We check the assumption of independence of  $\mathcal{L}$  with respect to  $A_0$  and  $\tan\beta$  with another  $m_0$ - $m_{1/2}$  scan at a different parameter point:  $A_0 = -200$  GeV and  $\tan\beta = 30$ , for illustration. The result is shown in Fig. 2b: the likelihood is similar to the one in Fig. 2a, and changing  $A_0$  and  $\tan\beta$  has not had a significant effect. Other constraints on parameters, such as those coming from having a charged lightest supersymmetric particle (shown by the blacked out region at the bottom of Fig. 2b) do display a significant  $\tan\beta$  and  $A_0$  dependence, but these are already taken into account within our fits and will not pose a problem. The very bottom of the plot has negative mass squared staus, and the signal rate could not be reliably calculated there. This has a slight effect on the interpolated 95% C.L. contour, and is responsible for it having an apparent (false) turning point in  $m_{1/2}$ . We shall quantify the effects of the  $\tan\beta - A_0$  independence assumption in our fits in Appendix A.

For increasing  $m_{1/2}$ , we see  $\Delta\chi^2$  reaching a constant in Fig. 2 because there is no SUSY signal, since squarks and gluinos become too heavy to be produced. At large  $m_0$  and small  $m_{1/2}$ , the SUSY signal is strongly dominated by gluino pair production, where the gluinos have three-body decays into squarks. Thus the dependence of  $\mathcal{L}$  on  $m_0$ , if it is above 1400 GeV, is negligible. We shall therefore model the likelihood as follows: we use



$s = 0$  for  $m_{1/2} > 500$  GeV. For  $m_0 > 1400$  GeV and  $m_{1/2} < 500$  GeV, we use the  $\mathcal{L}$  value given by the  $m_0 = 1400$  GeV line on the figure. For  $m_0 < 1400$  GeV and  $m_{1/2} < 500$  GeV, we interpolate linearly within the grid of likelihoods calculated.

### 3 Global CMSSM Fits Including the CMS $\alpha_T$ Search

We shall use a previous global Bayesian fit of the CMSSM from the KISMET collaboration [5] to: the relic density of dark matter, the anomalous magnetic moment of the muon, previous direct searches for sparticles, the branching ratios  $BR(b \rightarrow s\gamma)$ ,  $BR(B_s \rightarrow \mu\mu)$ ,  $M_W$ ,  $\sin^2 \theta_w^l$ , as well as 95% exclusions from LEP and Tevatron direct search data. In order to predict  $BR(b \rightarrow s\gamma)$ ,  $BR(B_s \rightarrow \mu\mu)$ , the dark matter relic density and the anomalous magnetic moment of the muon, micrOMEGAs1.3.6 [37, 38] was employed. It computes  $BR(b \rightarrow s\gamma)$  including one-loop SUSY corrections and NLO QCD corrections.  $BR(B_s \rightarrow \mu\mu)$  is calculated to one-loop. micrOMEGAs calculates the non Standard Model correction to the anomalous magnetic moment of the muon to one loop, and we added the dominant two-loop SUSY QED contributions from Ref. [39, 40]. SUSY-POPE [41], which includes SUSY contributions up to two loops, was used to calculate  $M_W$  and  $\sin^2 \theta_w$ . Spectral predictions from SOFTSUSY3.1.7 are used to place bounds from pre-LHC direct searches for sparticles and the lightest CP-even higgs boson. SOFTSUSY3.1.7 calculates the sparticle masses to two-loop in the renormalisation group equations, and one-loop in the threshold corrections. The dominant two-loop MSSM corrections are added to the Higgs mass computation, and a 2 GeV error on the prediction of  $m_h$  was assigned.

The ranges of input parameters considered were:  $2 < \tan \beta < 62$ ,  $|A_0|/\text{TeV} < 4$ ,  $60 < m_{1/2}/\text{GeV} < 2000$ ,  $60 < m_0/\text{GeV} < 4000$ . Variations with respect to the top mass  $m_t$ , the strong coupling constant  $\alpha_s(M_Z)$ , the fine structure constant  $\alpha(M_Z)$  and the bottom quark mass  $m_b(m_b)$  were all included. Various different prior distributions were examined in Ref. [5], but here we shall use the example of priors flat in the parameters listed above, except for  $m_0$  and  $m_{1/2}$ , which are flat in their logarithm. Using such log priors allows us to illustrate the effects of the  $\alpha_T$  search more acutely than with purely linear priors. Rigorous convergence criteria were satisfied by the fits, which were performed by ten Metropolis Markov Chains running simultaneously. For more details on the fits, we refer interested readers to Ref. [5].

The effect of the data is encoded within a likelihood function  $L(m)$  defined on model parameters  $m$ , and Bayesian inference consists of turning a prior probability distribution  $\pi(m)$  into a posterior probability distribution  $p(m|d)$  via Bayes' theorem  $p(m|d) = L(m)\pi(m)/D$ .  $D = \int dm L(m)\pi(m)$  is a constant over parameter space: the Bayesian evidence. Since we are performing parameter estimation, we are never interested in normalizing constants, because the inference is performed under the hypothesis that the model we are examining is correct and therefore the constants are always normalized such that the total posterior probability is 1. We take 2.7 million points from the Markov chain fits. The density of sampled points is proportional to the posterior probability density at any point. Each point  $i$  typically appears sampled several times, and we therefore set its weight  $\rho_G(p_i)$  equal to



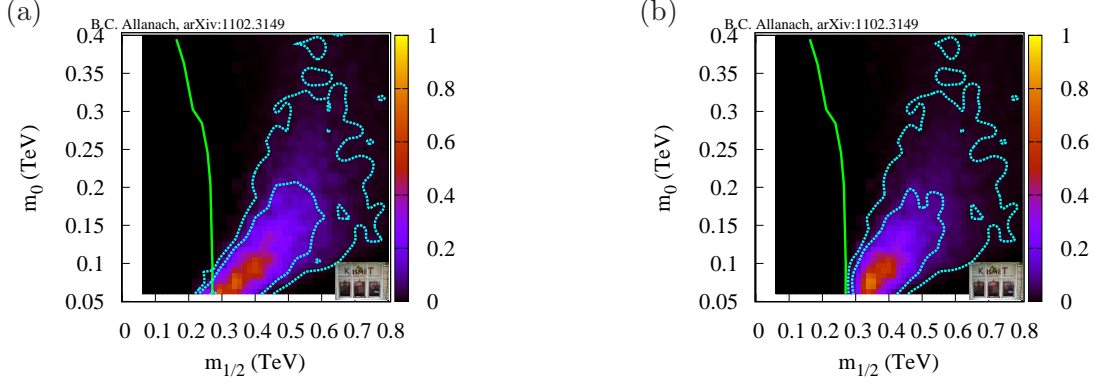


**Figure 3.** Global CMSSM fits: (a) excluding the CMS  $\alpha_T$  search and (b) including the CMS  $\alpha_T$  search likelihood. The posterior probability of each bin is shown as the background colour, normalized to the maximum bin probability. The almost vertical curve shows our approximation to the CMS 95% exclusion. The dotted cyan inner (outer) contour shows the 68% (95 %) Bayesian credibility region.

the number of times it appears. We write the point’s parameters as

$$p_i = \{m_0, A_0, m_{1/2}, \tan \beta, m_t, m_b(m_b), \alpha(M_Z), \alpha_s(M_Z)\}_i.$$

The Markov chain Monte Carlo statistically gives us proportionality of the weight with the posterior probability distribution  $p_G(p_i)$  (*prior* to the inclusion of LHC data) of the point:  $p_G(p_i) = k\rho_G(p_i)$ , where  $k$  is some constant which does not depend on  $p_i$ .

In order to take into account any new independent data with likelihood  $L_{new}(p_i)$ , we have the combined likelihood  $L_c(p_i) = L_{new}(p_i)L_G(p_i)$  which combines the global fit data with the new data. Thus the combined posterior probability density function is  $p_c(p_i) = cp_G(p_i)L_{new}(p_i)$ , where  $c$  is a constant that takes into account the fact that the Bayesian evidence changes through the introduction of new data. In terms of the Markov chain Monte Carlo point list, we obtain that  $p_c(p_i) = ck\rho_G(p_i)L_{new}(p_i)$ . Ignoring the constants, we therefore calculate the new posterior by re-weighting each point, multiplying its weight by the likelihood of the CMS  $\alpha_T$  search in Eq. 2.4. By plotting the posterior probability distributions before and after the  $\alpha_T$ -re-weighting, we can then examine the effect of the  $\alpha_T$  exclusion data on the CMSSM fits.

We show the fits marginalized over all parameters except for  $m_0$  and  $m_{1/2}$  in Fig. 3. In order to guide the eye, we have added the 95% exclusion contour (the light, almost vertical curve), but we remind the reader that the  $\alpha_T$  likelihood was taken into account, not just a veto from this curve. Nevertheless, we see in the figure the expected behavior: there is a small volume of good fit towards the bottom left of the plot that is “chopped off” by the  $\alpha_T$  exclusion limit. There are also non-trivial effects on the parameter plane: we see from Fig. 2a that there is a slight  $\sim 1\sigma$  preference of the data against high  $m_{1/2}$ , since there was an excess of observed events versus expected background. Such effects are present in the plot, but are easier to see when the posterior probability density is marginalized down to one dimension only (see below).

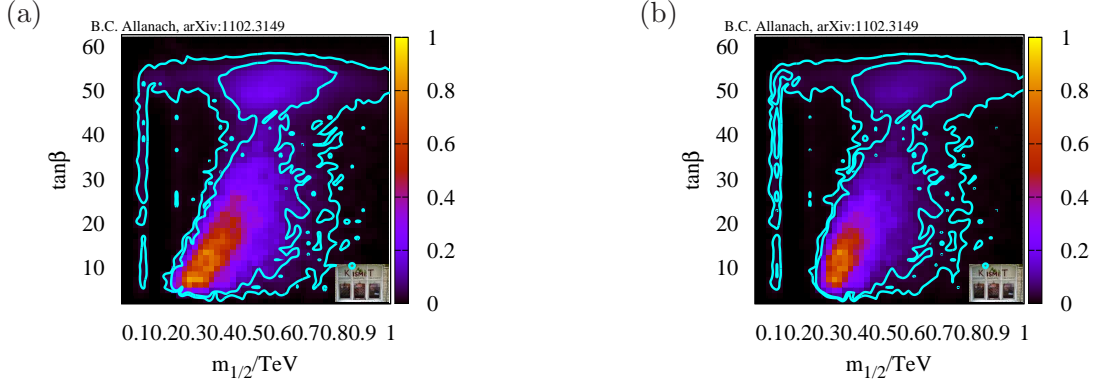


**Figure 4.** Global CMSSM fits: (a) excluding the CMS  $\alpha_T$  search and (b) including the CMS  $\alpha_T$  search likelihood. The posterior probability of each bin is shown as the background colour, normalized to the maximum bin probability. The dotted cyan inner (outer) contour shows the 68% (95 %) Bayesian credibility region.

We show the marginalization to the  $m_{1/2} - \tan\beta$  plane in Fig. 4. Here, we start to see the effect of non-trivial correlations of the CMSSM parameters from the indirect fits. The long, thin vertical region on the left-hand side of the figure corresponds to the  $h$ -pole region, where  $m_{\chi_1^0} \approx m_h/2$  and the lightest neutralinos  $\chi_1^0$  efficiently annihilate in the early universe through the  $s$ -channel higgs ( $h$ ) pole [42]. This region is at large values of  $m_0 > 1400$  GeV and low  $m_{1/2}$  [43]. Examining Fig. 2a, we see that this region is given a likelihood enhancement by the  $\alpha_T$  search, and we see evidence for this in Fig. 4b: it gains some 68% level contours as its probability mass increases. Also, the region at high  $\tan\beta$  within the 68% level contour has some of its probability mass removed, since it is at large values of  $m_{1/2}$ , where there is a slight  $\chi^2$  penalty compared to smaller values of  $m_{1/2} < 400$  GeV, due to the  $\alpha_T$   $1\sigma$  excess of events.

We display the probability distributions of the individual CMSSM parameters marginalized over all other parameters in Fig. 5. We see from Fig. 5a that, because of correlations between the parameters in the global fit, the  $\alpha_T$ -search slightly prefers values of  $m_0 \sim 100$  GeV. This is because the small  $m_{1/2}$  region is boosted by the  $1\sigma$  excess in the number of observed events, which also has a small  $m_0$  in order to obtain sufficient neutralino annihilation in the early universe (in the stau Co-annihilation region). Fig. 5b shows that small values of  $m_{1/2}$  are relatively disfavored by the  $\alpha_T$  search, except for the spike at  $m_{1/2} \approx 120$  GeV which corresponds to the  $h$ -pole region and is enhanced by including the  $\alpha_T$  search. Intermediate values of  $m_{1/2}$  of  $300 - 500$  are also relatively favored compared to larger values. The  $A_0$  distribution is relatively untouched by the search, as shown in Fig. 5c, whereas intermediate values of  $\tan\beta = 8 - 20$  are slightly preferred by it: see Fig. 5d.

Next, we turn to the effect of the  $\alpha_T$  search on sparticle masses. We plot the posterior probability distributions of a representative sample of four different masses in Fig. 6. The right handed squark mass  $m_{qR}$  is squeezed somewhat toward intermediate values of 600-1200 GeV by the  $\alpha_T$  search, as shown in Fig. 6a. A similar effect is found in the right-handed

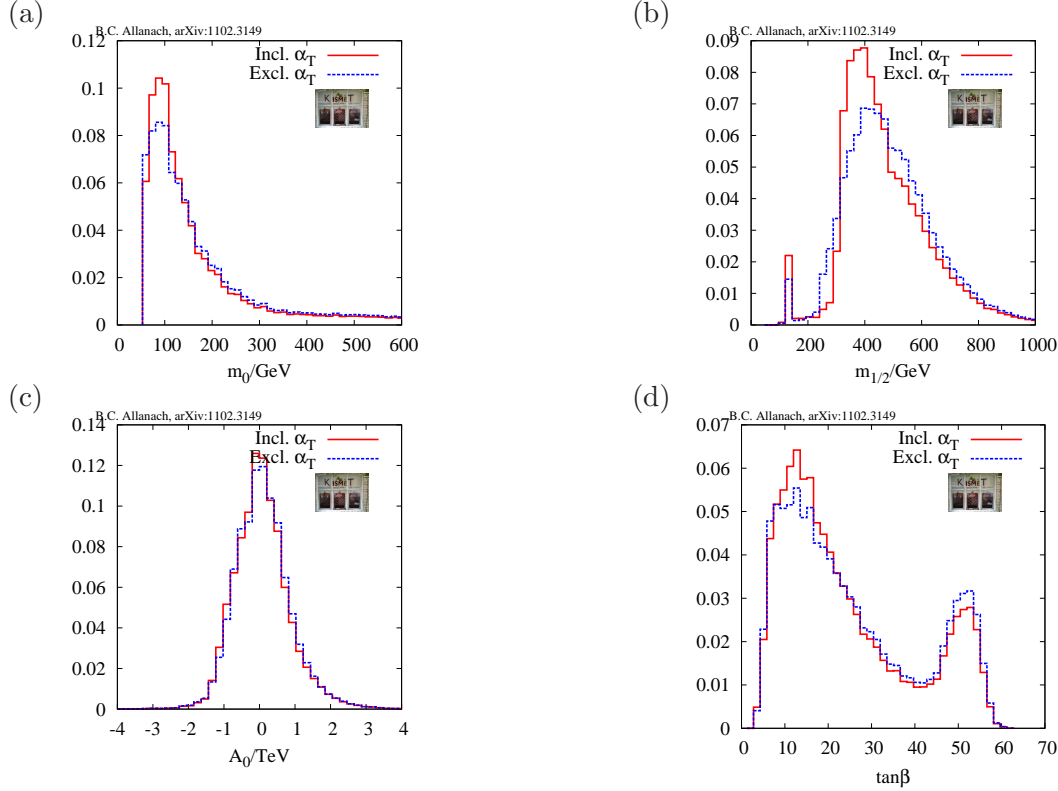


**Figure 5.** Effect of the  $\alpha_T$ -search on one dimensional probability distributions of CMSSM parameters. The area of each histogram has been normalized to 1 and labeled ‘Incl.  $\alpha_T$ ’ (‘Excl.  $\alpha_T$ ’) if it includes (excludes) the CMS  $\alpha_T$  search.

selectron mass  $m_{e_R}$ , which is squeezed somewhat toward intermediate values of 160-200 GeV, as shown in Fig. 6d.  $m_{\chi_1^0}$  and the gluino mass  $m_g$  are correlated strongly with  $m_{1/2}$  and Figs. 6b,c show that the overall features follow those of the  $m_{1/2}$  distribution: a spike corresponding to the  $h$ -pole at light masses and an enhancement of intermediate values of the masses to the detriment of more extreme values.

The probability distributions of masses found predict a probability distribution for the cross-section of sparticle production at the LHC. Approximately  $1 \text{ fb}^{-1}$  of integrated luminosity is expected to be collected over the next year at the LHC. Thus, a “weather forecast” of whether it will be raining particles (or whether we shall find a SUSY desert), is of special interest. We calculate the total sparticle production cross-section  $\sigma_{SUSY}$  predicted by our fits at the LHC, with no cuts or modelling of detector effects. This quantity then provides a crude upper bound on the actual SUSY signal cross-section that may be observed. However, we do not attempt here to quantify the probability of SUSY discovery in the next year, since such an inference is not yet robust due to the insufficient constraining power of the data. It appears from Fig. 7 that the prospects for SUSY discovery next year marginally improve after the inclusion of the  $\alpha_T$  search results.

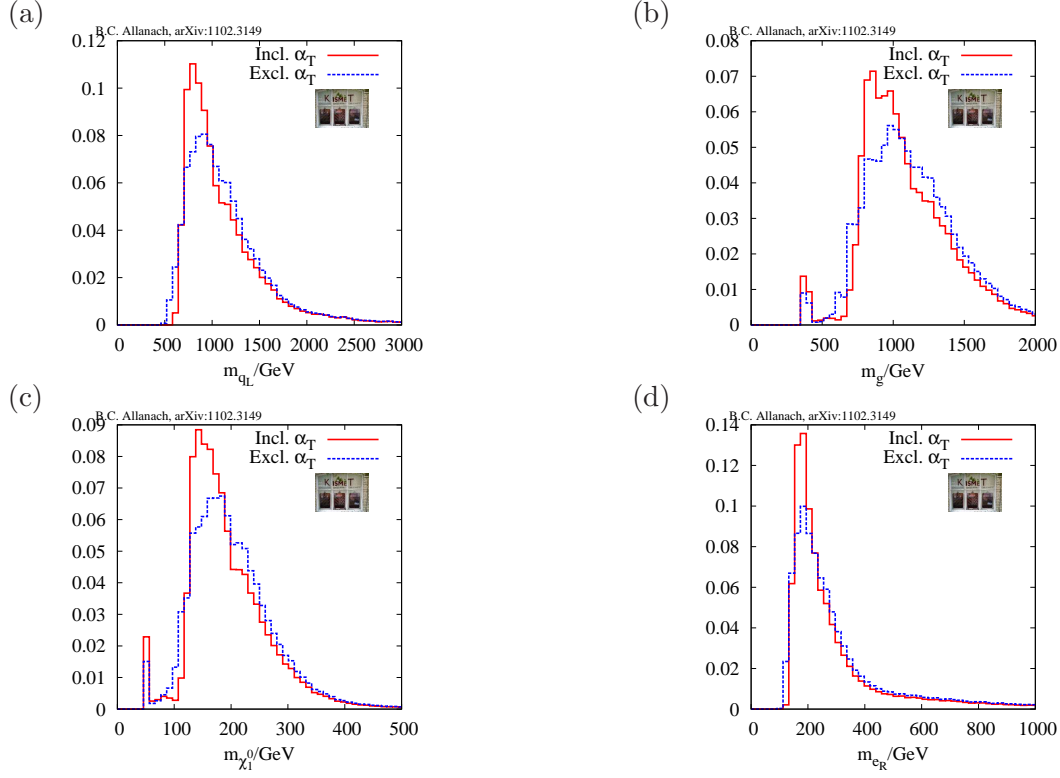


**Figure 6.** Effect of the  $\alpha_T$ -search on the probability distributions of sparticle masses in the CMSSM. The area of each histogram has been normalized to 1 and labeled ‘Incl.  $\alpha_T$ ’ (‘Excl.  $\alpha_T$ ’) if it includes (excludes) the CMS  $\alpha_T$  search.

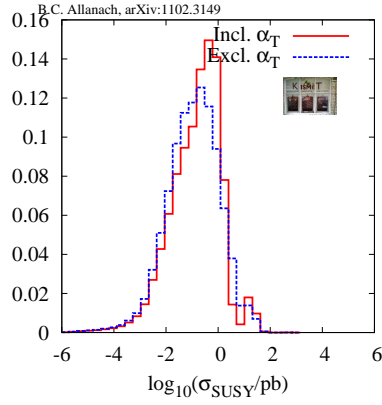


**Figure 7.** Effect of the  $\alpha_T$ -search on the total SUSY cross-section  $\sigma_{SUSY}$  in the CMSSM in  $pp$  collisions at  $\sqrt{s} = 7$  TeV. The area of each histogram has been normalized to 1 and labeled ‘Incl.  $\alpha_T$ ’ (‘Excl.  $\alpha_T$ ’) if it includes (excludes) the CMS  $\alpha_T$  search.

## 4 Summary and Conclusions

The CMS  $\alpha_T$  search has significantly extended the previous exclusion limits in the CMSSM. We have examined its effect on global fits of the CMSSM to the anomalous magnetic moment of the muon, the dark matter relic density and electroweak observables while taking into account previous direct searches for supersymmetric particles and Higgs bosons. The search nibbles away at the part of the parameter space where both squarks and gluinos are light, but also has some other non-trivial effects. Because the search saw a slight excess, intermediate masses acquire a small relative preference, with associated effects on  $\tan\beta$  because of parameter correlations in the global fit.

It is remarkable that even with the crudest of detector simulations (consisting of  $p_T$  and  $\eta$  cuts), and leading-order event generation, our 95% exclusion contour in a certain CMSSM parameter plane is close to CMS’s more sophisticated treatment. However, in order to be sure that we approximately reproduce the CMS likelihood elsewhere in parameter space, we require more details from the experimental publication. *We strongly advocate that the experiments publish more detail in order to allow more detailed checks: at least additional confidence level contours or, even better, the likelihood across a parameter plane, or ideally a RooStats workspace.*

As this work was being completed, ATLAS produced a search for jets, one lepton and missing transverse momentum [44] which extends the exclusion in the CMSSM plane as compared to the CMS search that we consider. The ATLAS search has an observed number of events lower than the expectation due to SM background (although the measurement is statistically compatible with the background). We leave the inclusion of this data to a future publication: it is likely to be computationally more difficult to include in our fits than the ones contained in the present paper because the signal rate may well have a dependence on all of the CMSSM parameters. Event simulation is a CPU-time bottle neck, and if it depends on more than just two or three parameters, is likely to need to be repeated for different sampled fit points since it couldn’t be easily interpolated in a reasonable amount of CPU time anyway. The ATLAS data will thus require other more computationally intensive techniques to analyze. Some of the effects that we have observed from the  $\alpha_T$  CMS search, such as an enhancement of intermediate values of sparticle masses due to the slight excess of events, will presumably be reversed when the recent ATLAS data is taken into account.

### A Validation of $\tan\beta - A_0$ Independence of the Likelihood

We now wish to check our approximation that the likelihood  $\mathcal{L}$  is independent of the other CMSSM parameters in the fit aside from  $m_0$  and  $M_{1/2}$ . In order to do this, we first take one hundred different sampled points at random from the 2.7 million different points in the fits, before the likelihood has been re-weighted by the  $\alpha_T$ -search. Each point has different Standard Model and CMSSM parameters, and the probability of selecting it is proportional to its posterior probability density of the fit to indirect data. These points therefore represent a faithful sampling from the fit, and we may estimate different

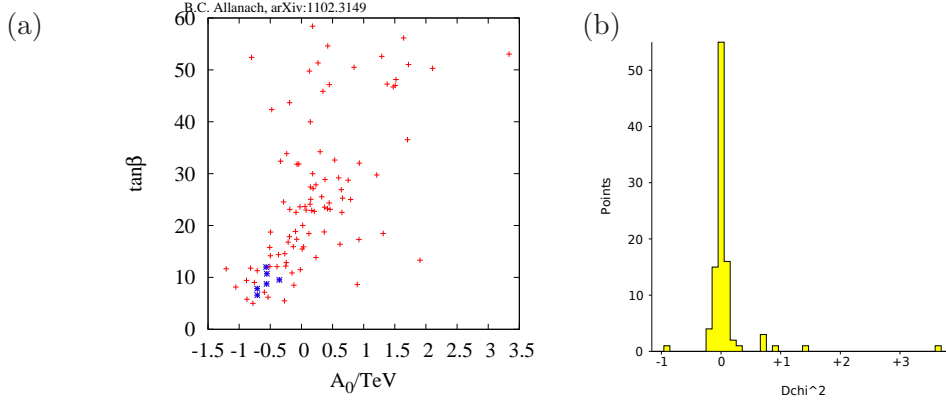


**Figure 8.** Check of the independence of the likelihood with respect to  $\tan \beta$  and  $A_0$  in the CMSSM fits. (a)  $A_0$  and  $\tan \beta$  values of the sampled points, (b) binned distribution of  $D\chi^2$ , the difference between the  $\Delta\chi^2$  calculated by our  $A_0 - \tan \beta$  independent approximation and the  $\Delta\chi^2$  calculated by event generation.

quantities by calculating their probability distributions from this faithful sampling. We show, for reference, the values of  $A_0$  and  $\tan \beta$  of the sampled points in Fig. 8a. For each of these points, we generate 10 000 SUSY signal events and estimate the numbers of events passing cuts in the  $\alpha_T$  search, as in section 2, turning the number of events into a  $\Delta\chi^2$  for the search. We then compare this  $\Delta\chi^2$  obtained by simulating events with the one from the linear interpolation of  $A_0 = 0$ ,  $\tan \beta = 3$  in Fig. 2a. The difference between the two,  $D\chi^2$ , measures how much our approximation is violated.

In Fig. 8b, we bin in  $D\chi^2$ , showing how many of the 100 points lie in each bin. Up to an overall normalization of  $1/100$  then, this is an estimate of the probability distribution of  $D\chi^2$  in our fit. All of the 100 points sampled have  $D\chi^2 < 0.2$  except for six, which are shown by asterisks in Fig. 8a. The most egregious has  $D\chi^2 = 3.7$ , but is heavily ruled out by the  $\alpha_T$ -search, with a  $\Delta\chi^2$  of 15. The others all have  $m_0 < 100$  GeV,  $m_{1/2} \sim 300$  GeV,  $\tan \beta \in (5, 10)$  and  $A_0 \in (-0.5, -1.0)$  TeV. The fact that the egregious points are clustered in parameter space can be understood as follows. The large values of  $-A_0$  at small  $m_0$  and  $m_{1/2}$  significantly change the up and down squark masses at these points compared to  $A_0 = 0$  via the MSSM renormalisation group equations (RGEs)<sup>3</sup>, having a resultant effect on the overall cross-section and hence on the number of SUSY signal events passing cuts. Negative  $A_0$  is preferred by the global fit as compared to positive  $A_0$  because it tends to give larger lightest CP-even Higgs masses by enhancing the stop mixing and enhancing the (dominant) stop loop correction to the Higgs mass. Once small  $m_{1/2}$  has been selected, the global fits preferentially select  $\tan \beta \in (5, 10)$ , as Fig. 4a shows. The anomalous magnetic moment of the muon prefers these values of  $\tan \beta$  for such light sparticles. For small  $m_0$  and  $m_{1/2}$ ,  $A_0 < -1$  TeV results in negative stau mass squared parameters, resulting in a charge breaking minimum of the scalar potential. Such values are therefore disallowed in

<sup>3</sup>The trilinear couplings enter the RGEs for the SUSY breaking masses of the Higgs bosons, which then enter the RGEs of the first two families of squarks.

the global fit.

We conclude that the assumed independence to parameters other than  $m_0$  and  $m_{1/2}$  is quite a good approximation, since, excluding the most egregious point (which is ruled out anyway), we obtain  $D\chi^2 = 0.04 \pm 0.22$ .

## Acknowledgments

This work has been partially supported by STFC. We thank other members of the Cambridge SUSY working group for discussions held, particularly C Lester and S Williams on  $\alpha_T$ . We thank D Grellscheid and P Richardson for communication regarding Herwig++, and F Moortgat and K Matchev for providing details of the CMS analysis.

## References

- [1] B. C. Allanach and C. G. Lester, *Multi-Dimensional mSUGRA Likelihood Maps*, *Phys. Rev.* **D73** (2006) 015013, [[hep-ph/0507283](#)].
- [2] B. C. Allanach, *Naturalness priors and fits to the constrained minimal supersymmetric standard model*, *Phys. Lett.* **B635** (2006) 123–130, [[hep-ph/0601089](#)].
- [3] R. Trotta, R. R. de Austri, and L. Roszkowski, *Prospects for direct dark matter detection in the constrained MSSM*, *New Astron. Rev.* **51** (2007) 316–320, [[astro-ph/0609126](#)].
- [4] B. C. Allanach, C. G. Lester, and A. M. Weber, *The Dark Side of mSUGRA*, *JHEP* **12** (2006) 065, [[hep-ph/0609295](#)].
- [5] B. C. Allanach, K. Cranmer, C. G. Lester, and A. M. Weber, *Natural Priors, CMSSM Fits and LHC Weather Forecasts*, *JHEP* **08** (2007) 023, [[0705.0487](#)].
- [6] L. Roszkowski, R. R. de Austri, J. Silk, and R. Trotta, *On prospects for dark matter indirect detection in the Constrained MSSM*, *Phys. Lett.* **B671** (2009) 10–14, [[0707.0622](#)].
- [7] B. C. Allanach and D. Hooper, *Panglossian Prospects for Detecting Neutralino Dark Matter in Light of Natural Priors*, *JHEP* **10** (2008) 071, [[0806.1923](#)].
- [8] F. Feroz *et. al.*, *Bayesian Selection of sign( $\mu$ ) within mSUGRA in Global Fits Including WMAP5 Results*, *JHEP* **10** (2008) 064, [[0807.4512](#)].
- [9] O. Buchmueller *et. al.*, *Predictions for Supersymmetric Particle Masses in the CMSSM using Indirect Experimental and Cosmological Constraints*, *JHEP* **09** (2008) 117, [[0808.4128](#)].
- [10] R. Trotta, F. Feroz, M. P. Hobson, L. Roszkowski, and R. Ruiz de Austri, *The Impact of priors and observables on parameter inferences in the Constrained MSSM*, *JHEP* **12** (2008) 024, [[0809.3792](#)].
- [11] L. Roszkowski, R. Ruiz de Austri, R. Trotta, Y.-L. S. Tsai, and T. A. Varley, *Global fits of the Non-Universal Higgs Model*, [0903.1279](#).
- [12] F. Feroz, M. P. Hobson, L. Roszkowski, R. Ruiz de Austri, and R. Trotta, *Are  $BR(b \rightarrow s \gamma)$  and  $(g - 2)_\mu$  consistent within the Constrained MSSM?*, [0903.2487](#).
- [13] D. E. Lopez-Fogliani, L. Roszkowski, R. R. de Austri, and T. A. Varley, *A Bayesian Analysis of the Constrained NMSSM*, *Phys. Rev.* **D80** (2009) 095013, [[0906.4911](#)].
- [14] L. Roszkowski, R. Ruiz de Austri, and R. Trotta, *Efficient reconstruction of CMSSM parameters from LHC data - A case study*, *Phys. Rev.* **D82** (2010) 055003, [[0907.0594](#)].



- [15] O. Buchmueller *et. al.*, *Likelihood Functions for Supersymmetric Observables in Frequentist Analyses of the CMSSM and NUHM1*, *Eur. Phys. J.* **C64** (2009) 391–415, [[0907.5568](#)].
- [16] O. Buchmueller *et. al.*, *Predictions for  $m_t$  and  $m_W$  in Minimal Supersymmetric Models*, *Phys. Rev.* **D81** (2010) 035009, [[0912.1036](#)].
- [17] H. Baer, S. Kraml, A. Lessa, S. Sekmen, and X. Tata, *Effective Supersymmetry at the LHC*, *JHEP* **10** (2010) 018, [[1007.3897](#)].
- [18] O. Buchmueller *et. al.*, *Frequentist Analysis of the Parameter Space of Minimal Supergravity*, [1011.6118](#).
- [19] B. C. Allanach and C. G. Lester, *Sampling using a 'bank' of clues*, *Comput. Phys. Commun.* **179** (2008) 256–266, [[0705.0486](#)].
- [20] F. Feroz, M. P. Hobson, and M. Bridges, *MultiNest: an efficient and robust Bayesian inference tool for cosmology and particle physics*, [0809.3437](#).
- [21] F. Feroz, K. Cranmer, M. Hobson, R. R. de Austri, and R. Trotta, *Challenges of Profile Likelihood Evaluation in Multi- Dimensional SUSY Scans*, [1101.3296](#).
- [22] M. Bridges *et. al.*, *A Coverage Study of the CMSSM Based on ATLAS Sensitivity Using Fast Neural Networks Techniques*, [1011.4306](#).
- [23] B. C. Allanach, M. J. Dolan, and A. M. Weber, *Global Fits of the Large Volume String Scenario to WMAP5 and Other Indirect Constraints Using Markov Chain Monte Carlo*, *JHEP* **08** (2008) 105, [[0806.1184](#)].
- [24] S. S. AbdusSalam, B. C. Allanach, M. J. Dolan, F. Feroz, and M. P. Hobson, *Selecting a Model of Supersymmetry Breaking Mediation*, *Phys. Rev.* **D80** (2009) 035017, [[0906.0957](#)].
- [25] S. S. AbdusSalam, B. C. Allanach, F. Quevedo, F. Feroz, and M. Hobson, *Fitting the Phenomenological MSSM*, *Phys. Rev.* **D81** (2010) 095012, [[0904.2548](#)].
- [26] **CMS** Collaboration, V. Khachatryan *et. al.*, *Search for Supersymmetry in  $pp$  Collisions at 7 TeV in Events with Jets and Missing Transverse Energy*, [1101.1628](#).
- [27] A. Strumia, *The fine-tuning price of the early LHC*, [1101.2195](#).
- [28] D. S. M. Alves, E. Izaguirre, and J. G. Wacker, *It's On: Early Interpretations of ATLAS Results in Jets and Missing Energy Searches*, [1008.0407](#).
- [29] L. Randall and D. Tucker-Smith, *Dijet Searches for Supersymmetry at the LHC*, *Phys. Rev. Lett.* **101** (2008) 221803, [[0806.1049](#)].
- [30] Z. Usubov, *Looking for Squark Pair Production in the Early LHC Data*, [1005.5062](#).
- [31] A. J. Barr and C. G. Lester, *A Review of the Mass Measurement Techniques proposed for the Large Hadron Collider*, *J. Phys.* **G37** (2010) 123001, [[1004.2732](#)].
- [32] M. Bahr *et. al.*, *Herwig++ Physics and Manual*, *Eur. Phys. J.* **C58** (2008) 639–707, [[0803.0883](#)].
- [33] B. C. Allanach, *SOFTSUSY: a program for calculating supersymmetric spectra*, *Comput. Phys. Commun.* **143** (2002) 305–331, [[hep-ph/0104145](#)].
- [34] M. Muhlleitner, A. Djouadi, and Y. Mambrini, *SDECAY: A Fortran code for the decays of the supersymmetric particles in the MSSM*, *Comput. Phys. Commun.* **168** (2005) 46–70, [[hep-ph/0311167](#)].
- [35] P. Z. Skands *et. al.*, *SUSY Les Houches Accord: Interfacing SUSY Spectrum Calculators*,

- Decay Packages, and Event Generators*, *JHEP* **07** (2004) 036, [[hep-ph/0311123](#)].
- [36] M. Cacciari and G. P. Salam, *Dispelling the  $N^3$  myth for the  $k_t$  jet-finder*, *Phys. Lett.* **B641** (2006) 57–61, [[hep-ph/0512210](#)].
  - [37] G. Belanger, F. Boudjema, A. Pukhov, and A. Semenov, *MicrOMEGAs: A Program for calculating the relic density in the MSSM*, *Comput.Phys.Commun.* **149** (2002) 103–120, [[hep-ph/0112278](#)].
  - [38] G. Belanger, F. Boudjema, A. Pukhov, and A. Semenov, *micrOMEGAs: Version 1.3*, *Comput.Phys.Commun.* **174** (2006) 577–604, [[hep-ph/0405253](#)].
  - [39] S. Heinemeyer, D. Stockinger, and G. Weiglein, *Two loop SUSY corrections to the anomalous magnetic moment of the muon*, *Nucl.Phys.* **B690** (2004) 62–80, [[hep-ph/0312264](#)].
  - [40] S. Heinemeyer, D. Stockinger, and G. Weiglein, *Electroweak and supersymmetric two-loop corrections to  $(g-2)(\mu)$* , *Nucl.Phys.* **B699** (2004) 103–123, [[hep-ph/0405255](#)].
  - [41] S. Heinemeyer, W. Hollik, D. Stockinger, A. Weber, and G. Weiglein, *Precise prediction for  $M(W)$  in the MSSM*, *JHEP* **0608** (2006) 052, [[hep-ph/0604147](#)].
  - [42] M. Drees and M. M. Nojiri, *The Neutralino relic density in minimal  $N = 1$  supergravity*, *Phys.Rev.* **D47** (1993) 376–408, [[hep-ph/9207234](#)].
  - [43] A. Djouadi, M. Drees, and J.-L. Kneur, *Neutralino dark matter in mSUGRA: Reopening the light Higgs pole window*, *Phys.Lett.* **B624** (2005) 60–69, [[hep-ph/0504090](#)].
  - [44] **ATLAS** Collaboration, G. Aad *et. al.*, *Search for supersymmetry using final states with one lepton, jets, and missing transverse momentum with the ATLAS detector in  $\sqrt{s} = 7$  TeV  $pp$* , [1102.2357](#).